



## Search for Resonant Slepton Production via the $LQ\bar{D}$ Coupling $\lambda'_{211}$

The DØ Collaboration  
URL <http://www-d0.fnal.gov>  
(Dated: August 10, 2004)

This note documents the search for R-parity violating production and decay of charged sleptons. Assuming a non zero  $LQ\bar{D}$  coupling  $\lambda'_{211}$  leads to final states with two jets and at least two muons. We perform a search using 153.8/pb of integrated luminosity collected between standard model expectation, and cross section limits as a function of  $m_{\tilde{\chi}_1^0}$  and  $m_{\tilde{\mu}}$  are set for  $\lambda'_{211} = 0.07$ .

*Preliminary Results for Summer 2004 Conferences*

## I. INTRODUCTION

The R-parity violating ( $\mathcal{R}_p$ ) extension of the MSSM contains additional terms in the superpotential, which are trilinear in the quark and lepton superfields,

$$W_{\mathcal{R}_p} = \sum_{i,j,k} \left( \frac{1}{2} \lambda_{ijk} L_i L_j E_k^c + \lambda'_{ijk} L_i Q_j D_k^c + \frac{1}{2} \lambda''_{ijk} U_i^c D_j^c D_k^c \right), \quad (1)$$

where  $i, j, k$  are family indices. These  $\mathcal{R}_p$  couplings offer the opportunity to produce the scalar supersymmetric particles as resonances [2]. This is not allowed in the  $R_p$  conserving supersymmetric models where sparticles must be produced in pairs. Although the  $\mathcal{R}_p$  coupling constants are constrained by the low-energy experimental bounds [3, 4], the resonant superpartner production might reach high cross sections both at lepton and hadron colliders [5, 6].

At hadron colliders, either a sneutrino ( $\tilde{\nu}$ ) or a charged slepton ( $\tilde{l}$ ) can be produced in resonance via the  $\lambda'_{ijk}$  coupling. For most of the SUSY models, the slepton produced at the resonance has two possible decays, namely a decay into either a chargino or a neutralino. Therefore, in the scenario of a single dominant  $\lambda'_{ijk}$  coupling and for most of the SUSY models, either a single chargino or a neutralino is produced together with either a charged lepton or a neutrino, through the resonant superpartner production at hadron colliders. There are thus four main possible types of single superpartner production reactions involving  $\lambda'_{ijk}$  at hadron colliders which receive a contribution from resonant SUSY particle production.

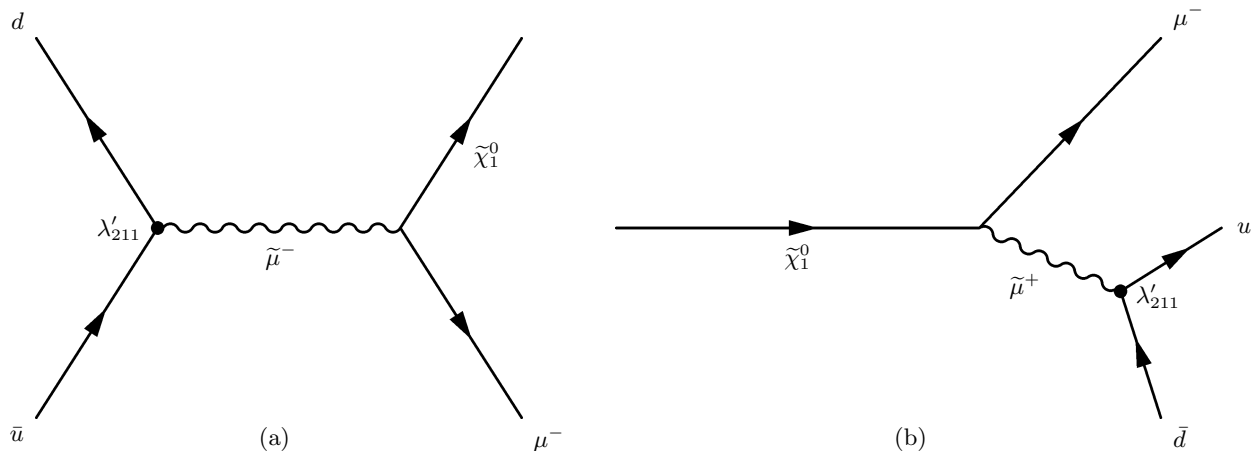


FIG. 1: Resonant smuon production and neutralino decay via  $\lambda'_{211}$ .

In the analysis presented here, only the resonant production of a smuon is considered (Fig. 1a), which leads to a final state with two muons and two jets: the smuon can decay into a muon and a neutralino, which decays into two jets and a muon (Fig. 1b). The resonant sneutrino production would lead to final states with missing transverse energy. The order of magnitude of the resonant production cross sections is comparable, however the final states are not. This analysis takes advantage of the ability to reconstruct the neutralino and smuon mass which is not possible with neutrinos in the final state. Nevertheless will the final state with missing  $E_T$  be added to this analysis in the future.

All given cross sections and limits in this note refer to the smuon production cross section times branching ratio into a neutralino and muon. The  $\lambda'_{ijk}$  coupling allows neutralino decays via virtual sparticles as muon sneutrino, smuon and squarks into two 1<sup>st</sup> generation quarks and one second generation lepton. This leads to a signal inefficiency of approx. 50%, since we only consider the final state with two muons and without neutrinos. The quark or muon produced at the neutralino decay vertex is of very low  $p_T$ , since the simultaneously produced sparticle (smuon or squark) is highly virtual. It is impossible to detect on an event by event basis which neutralino decay topology takes place, since the possible topologies — into a quark / squark pair or into a muon / smuon pair (Fig. 1b) — share the same final state and interfere therefore coherently. We use the minimal supergravity framework (mSUGRA) for SUSY breaking.

While the analysis shares common aspects with the Run I analysis [1], it also benefits greatly from the improved tracking capabilities and a better sensitivity of the Run II detector.

## II. DATA SETS AND EVENT SELECTION

The search uses Run II data collected between April 2002 and September 2003. “Bad runs” for the muon systems, calorimeter, jets, MET, CFT, and bad luminosity blocks have been excluded, as well as duplicate events. Each event has to be accepted by one of several di-muon trigger.

The data sample corresponds to an integrated luminosity of  $153.8 \pm 10.0 \text{ pb}^{-1}$ .

### A. Event Pre-Selection

The preselected sample consists of two muons with at least 2 wire chamber hits and one scintillator hit before and after the toroid iron, a transverse momentum of at least 20 GeV and 8 GeV, and two jets with minimum  $E_T$  of 15 GeV, reconstructed with a cone algorithm ( $\Delta R = \sqrt{\Delta\phi^2 + \Delta\eta^2} = 0.5$ ). Also, either the second jet or the second muon of each event is required to have a minimum  $p_T$  of 20 GeV, since only one of the three particles from the neutralino decay has very low energy (the one produced together with the virtual squark or smuon, directly at the neutralino decay vertex).

Both muons are required to be isolated, so that the sum of the transverse energy in calorimeter cells in a hollow cone ( $R = 0.4$ ,  $r = 0.1$ ) along the muon track does not exceed 2.5 GeV, and the sum of the transverse momenta of tracks in a cone with radius  $\sqrt{\phi^2 + \eta^2} = 0.5$  is smaller than 2.5 GeV. Both muons are also required to match a track in the central tracking system. Remaining cosmic muons are rejected by cutting on the scintillator timing.

Each jet is required to have a distance from any muon in  $\Delta R$  greater than 0.5. The separation between the two muons is required to be larger than  $\Delta R = 1.0$ . This muon separation requirement is found to reject nearly all remaining Standard Model QCD events without reducing the signal efficiency. Since little missing transverse energy is expected, we require  $\cancel{E}_T < 60 \text{ GeV}$ .

In  $153.8 \text{ pb}^{-1}$  of data, 258 events match these criteria.

### B. Event Selection

To separate the Standard Model background from the signal, additional topological cuts are applied. The  $p_T$  threshold for the next to leading muon is raised to 10 GeV (**cut 2**, Fig. 2d) and the sum of the muon transverse momenta is required to be greater than 60 GeV (**cut 3**). The  $p_T$  cut on the leading jet is raised to 25 GeV (**cut 5**, Fig. 2b)

Angular separations  $\Delta R$  are used to remove any remaining QCD or heavy flavor backgrounds, and to enhance the specific decay channel of interest. The highest  $p_T$  muon is nearly always created at the decay vertex of the resonant produced slepton and the highest jet at the  $LQ\bar{D}$  decay of the virtual sparticle as explained in section I. The pseudorapidity of both jets is required to be in a region of well understood jet energy scale  $|\eta| < 2$  (**cut 10**).

Considering the slepton mass, which is usually more than twice the neutralino mass, it is understandable that e.g. the leading muon and the leading jet will be back to back.

**cut 6** : Separation between the two jets  $0.5 < \Delta R < 2.8$ ;

**cut 9** : Separation between leading muon and 1<sup>st</sup> jet  $2.1 < \Delta R < 4.1$ ;

Separation between leading muon and 2<sup>nd</sup> jet  $0.5 < \Delta R < 4.1$ ;

Separation between the next to leading muon and the 1<sup>st</sup>, 2<sup>nd</sup> jet  $0.5 < \Delta R < 2.5$ ;

In order to further enhance the signal, the following invariant masses are calculated: the invariant mass of the two muons to reject  $Z$  events ( $M_{\mu\mu}$ ); the invariant mass of the two muons and the two jets ( $M_{\bar{\mu}}$ ); and the invariant mass of the second leading muon and the two jets ( $M_{\bar{\chi}_0^1}$ ). Cuts depending on the SUSY parameter point under study are applied:

**cut 1** : For the leading muon,  $p_T > 21.25 \text{ GeV} + 15/80 \cdot (M_{\bar{\mu}} - M_{\bar{\chi}_0^1})$  (i.e.  $p_T > 51.4 \text{ GeV}$  for point #14, Fig. 2a);

**cut 4** : To reject  $Z$  events, we discard events with  $91 \text{ GeV} - (5 + M_{\bar{\chi}_0^1}/9) < M_{\mu\mu} < 91 \text{ GeV} + (5 + M_{\bar{\chi}_0^1}/9)$  (i.e.  $M_{\mu\mu} \in 91 \pm 16.4 \text{ GeV}$  for point #14, Fig. 2c);

**cut 7** : The neutralino candidate mass has to be within the range  $-40$  GeV and  $+20$  GeV of the theoretically expected value of the mSUGRA point under study (Fig. 2f);

**cut 8** : The smuon candidate is required to be reconstructed within 20% of its theoretically expected mass.

The cuts have been chosen such that on average for all considered parameter points the ratio  $S/\sqrt{B}$  ( $S$  final signal,  $B$  final background) is optimal.

After the preselection described in section II A, 258 events remain in the data, while  $270.5 \pm 8.0_{-77.0}^{+82.1}$  events are expected from Standard Model backgrounds. In Fig. 2 we show comparisons between data and Monte Carlo simulation; the data are reasonably well described by the simulation. A signal Monte Carlo sample (point #14), multiplied by 10, is plotted as well.

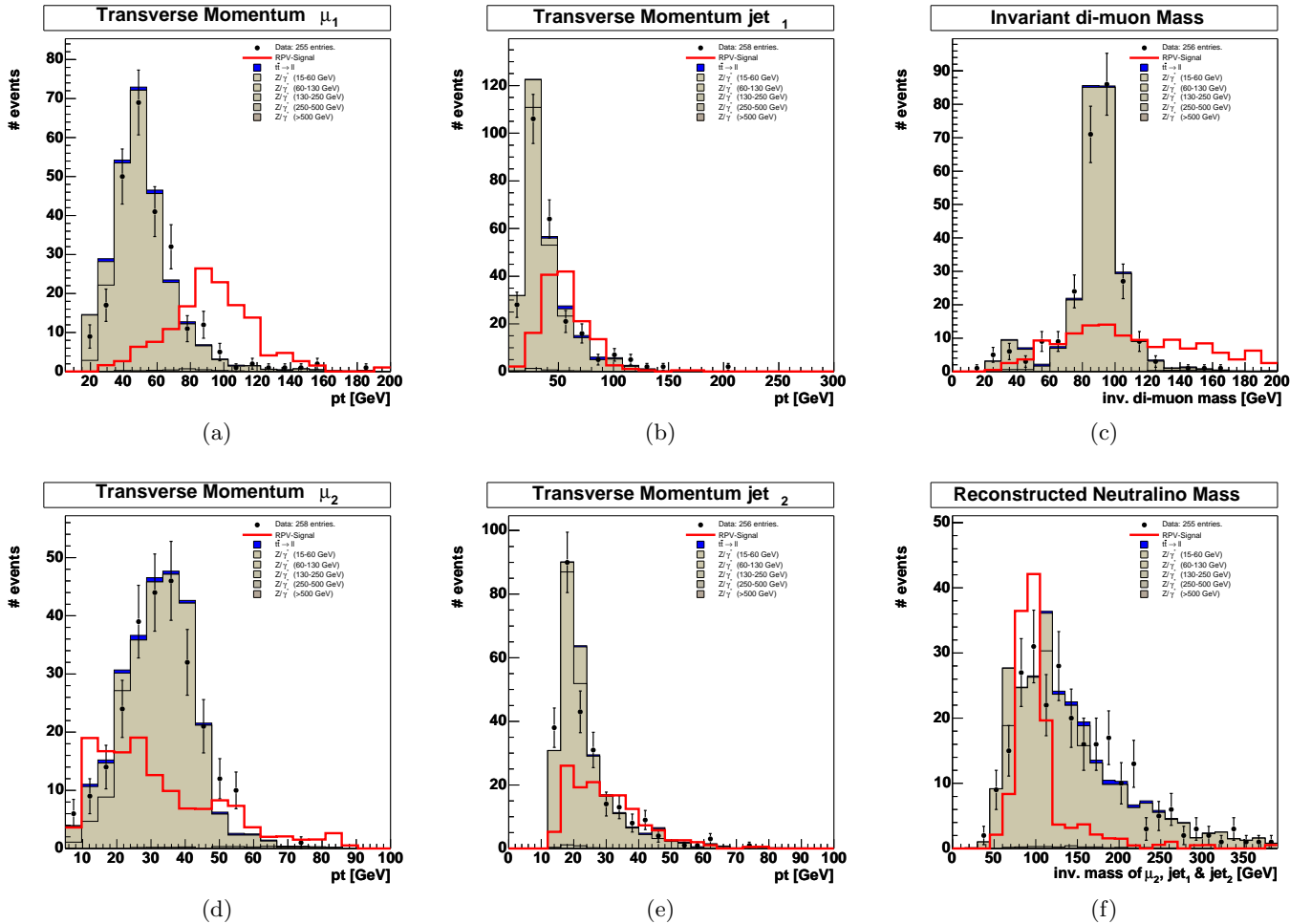


FIG. 2: Control distributions for the preselected sample: leading and second leading muon  $p_T$  (left), leading and second leading jet  $p_T$  (center), invariant di-muon mass (top right) and the reconstructed neutralino mass (bottom right). Data (points) are compared to the Standard Model expectation (brown and blue histograms). The signal (red line, point #14) is scaled up by a factor 10.

### C. Trigger Efficiencies

All Monte Carlo background and signal events have been weighted according to the event properties, like muon energy and angular distributions, in order to describe the di-muon trigger efficiency.

### III. MONTE CARLO SIMULATION

#### A. Background Monte Carlo

The dominant background is  $Z/\gamma^*+2\text{jet}$  production. Other Standard Model processes have also been considered.  $W+\text{jets}$ ,  $WZ$ ,  $WW$ ,  $ZZ$ ,  $b\bar{b}$ , and  $t\bar{t} \rightarrow l$  jets were found to be negligible.

The inclusive  $Z/\gamma^*$  process has been simulated with Pythia 6.2 [7], with a scale factor applied to correct for higher order effects [8]. This factor depends on the  $Z/\gamma^*$  mass and varies between 1.3 and 1.4.

#### B. Signal Monte Carlo

The signal Monte Carlo samples have been generated with Susygen v3.00-43 [9] and reconstructed mostly on the DØ workstation farm (Clued0) and on GridKa (Forschungszentrum Karlsruhe). In total 125k events with about 5000 events per point have been generated and passed through the full detector simulation. Events have been combined with Poisson distributed minimum bias events, 0.8 on average. The SUSY parameter space has been scanned with fixed smuon and neutralino masses.

For all points,  $\lambda'_{211}$  has been fixed to 0.07 which is for many considered points close to the limit given by previous analysis or theoretical constraints [1, 2]; only  $A_0 = 0$ ,  $\tan(\beta) = 2$ , and  $\text{sgn}(\mu) = -1$  are considered.

#### C. Detector Simulation

Several tests have been performed to check the validity of the detector simulation. Special care has been taken to correct the muon and jet momentum scale.

To account for the latest knowledge of the jet energy scale, corrections are applied to the data as well as to the Monte Carlo simulations. The missing energy is recalculated after these changes.

$$E_{corr} = \frac{E_{meas} - O}{R \times S}$$

where  $R$  is the calorimeter response to a jet,  $O$  is the energy offset and  $S$  is the fraction of calorimeter activity outside the jet cone.

A sample of dimuon events in the  $Z$  mass region ( $60 < M_{\mu\mu} < 120$  GeV) is used to calculate the isolation efficiency by a *tag and probe* method. Both muons were required to match with a central track and to have a minimal transverse momentum of 10 GeV. One muon must satisfy the isolation criteria. The isolation efficiency is the probability that the second muon is isolated, too. A  $p_T$  independent correction factor, which reflects the different isolation efficiencies in data and Monte Carlo, is estimated to be 0.942.

### IV. SYSTEMATIC UNCERTAINTIES

The uncertainty coming from the jet energy scale is derived by varying the jet  $E_T$  by one standard deviation, see also table I.

Effects of the imperfect detector simulation are considered together with the systematic error on the isolation (3%) and muon tracking and matching efficiency (<1%). Together a constant uncertainty of  $3\% \oplus 1\% \leq 4\%$  is estimated.

The uncertainty on the  $(Z/\gamma)^*$  production cross section is taken into account by varying the NNLO cross section correction [8] by one standard deviation. Part of the error is the uncertainty of the parton density functions.

uncertainty	tot. syst. error background	tot. syst. error signal
trigger	+5.3% / -6.9%	6% - 9%
$Z/\gamma^*$ cross section (k-factor)	+3.0% / -2.9%	—
jet energy scale	+30% / -27%	8% - 33%
Isolation & Tracking	+3.6% / -3.6%	+4% / -4%

TABLE I: Effect of the systematic uncertainties on the preselection background and signal Monte Carlo samples.

The luminosity uncertainty is 6.5%. A summary of the systematic errors can be found in table I.

#Cut	Cut type	Data	Signal	SM background	Signal Eff [%]
	preselection	258	$14.1 \pm 0.9^{+1.9}_{-2.0}$	$270.5 \pm 8.0^{+82.1}_{-77.0}$	$6.8 \pm 0.7$
1	mu1pt	125	$13.2 \pm 0.9^{+1.9}_{-1.9}$	$114.8 \pm 3.1^{+28.3}_{-27.2}$	$6.4 \pm 0.6$
2	mu2pt	123	$12.8 \pm 0.8^{+1.8}_{-1.8}$	$114.1 \pm 3.1^{+28.2}_{-27.1}$	$6.2 \pm 0.6$
3	muptsum	123	$12.8 \pm 0.8^{+1.8}_{-1.8}$	$114.1 \pm 3.1^{+28.2}_{-27.1}$	$6.2 \pm 0.6$
4	dimumass	24	$9.0 \pm 0.7^{+1.6}_{-1.5}$	$21.3 \pm 1.2^{+4.7}_{-5.1}$	$4.3 \pm 0.4$
5	jet1pt	20	$8.5 \pm 0.7^{+1.5}_{-1.4}$	$16.2 \pm 1.0^{+3.6}_{-2.5}$	$4.1 \pm 0.4$
6	jetangle	14	$7.8 \pm 0.7^{+1.4}_{-1.3}$	$9.9 \pm 0.8^{+2.5}_{-1.1}$	$3.8 \pm 0.4$
7	chimass2	5	$6.8 \pm 0.6^{+1.1}_{-1.3}$	$3.3 \pm 0.5^{+1.1}_{-0.3}$	$3.2 \pm 0.3$
8	smumass	2	$6.2 \pm 0.6^{+1.1}_{-1.7}$	$1.8 \pm 0.4^{+0.2}_{-0.3}$	$3.0 \pm 0.3$
9	$\Delta R(\mu_i, \text{jet}_j)$	2	$4.9 \pm 0.5^{+0.6}_{-1.2}$	$1.2 \pm 0.3^{+0.1}_{-0.2}$	$2.3 \pm 0.2$
10	eta jet <sub>i</sub>	2	$4.4 \pm 0.5^{+0.5}_{-1.1}$	$1.1 \pm 0.3^{+0.2}_{-0.2}$	$2.1 \pm 0.2$

TABLE II: Observed number of events after each selection cut, expected signal, and standard model expectation. Numbers are for signal point #14. The first error is the statistical uncertainty, the second error is the total systematic uncertainty.

#Cut	Cut type	Data	Signal	SM background	Signal Eff [%]
	preselection	258	$273.1 \pm 16.3^{+46.5}_{-54.4}$	$270.5 \pm 8.0^{+82.1}_{-77.0}$	$20.1 \pm 2.2$
1	mu1pt	225	$251.9 \pm 15.6^{+43.4}_{-52.0}$	$218.3 \pm 4.3^{+67.5}_{-62.6}$	$18.6 \pm 2.1$
2	mu2pt	221	$242.0 \pm 15.3^{+41.4}_{-48.3}$	$217.3 \pm 4.3^{+67.2}_{-62.5}$	$17.9 \pm 2.0$
3	muptsum	219	$232.8 \pm 15.0^{+39.6}_{-47.2}$	$215.0 \pm 4.3^{+65.4}_{-61.9}$	$17.2 \pm 1.9$
4	dimumass	41	$131.3 \pm 11.3^{+20.5}_{-22.5}$	$31.6 \pm 1.5^{+8.4}_{-8.2}$	$9.7 \pm 1.0$
5	jet1pt	30	$116.7 \pm 10.6^{+22.4}_{-23.3}$	$22.7 \pm 1.3^{+6.3}_{-4.0}$	$8.6 \pm 1.0$
6	jetangle	23	$97.7 \pm 9.7^{+16.8}_{-16.2}$	$13.5 \pm 1.0^{+3.4}_{-2.1}$	$7.2 \pm 0.8$
7	chimass2	8	$89.5 \pm 9.3^{+15.8}_{-12.9}$	$5.6 \pm 0.7^{+1.5}_{-0.7}$	$6.6 \pm 0.7$
8	smumass	3	$81.5 \pm 8.9^{+18.9}_{-17.2}$	$3.2 \pm 0.5^{+0.6}_{-0.4}$	$6.0 \pm 0.7$
9	$\Delta R(\mu_i, \text{jet}_j)$	1	$21.0 \pm 4.5^{+3.9}_{-5.9}$	$1.2 \pm 0.3^{+0.2}_{-0.1}$	$1.5 \pm 0.2$
19	eta jet <sub>i</sub>	1	$19.2 \pm 4.3^{+3.0}_{-4.9}$	$1.1 \pm 0.3^{+0.2}_{-0.1}$	$1.4 \pm 0.2$

TABLE III: Observed number of events after each selection cut, expected signal, and standard model expectation. Numbers are for signal point #12. The first error is the statistical uncertainty, the second error is the total systematic uncertainty.

## V. RESULTS

Since the event selection cuts vary with the signal point under study, we list here the number of selected events, standard model expectation, and signal expectation for two specific points in the SUSY parameter space (points #12 and #14). The results are given in tables II and III.

The total signal efficiency is typically 0.5%-6%. As an example, for point #14 and after all cuts, 2 events are observed with an expected background of  $1.1 \pm 0.3^{+0.2}_{-0.2}$ .

Reasonable agreement between the Standard Model expectation and the observed number of events is found for all parameter points. Some interesting points are listed in table IV.

We note that the SUSYGEN signal cross sections have not been corrected to account for higher order corrections.

### A. Signal Efficiency

As mentioned in section I, the signal efficiency suffers a loss of about 50% due to the possible decay of the neutralino into a neutrino and two jets instead of one muon and two jets. For most of the studied points the signal efficiency is between 1 % and 3 %. The efficiency drops for small neutralino masses since the neutralino mass affects directly the energy of both jets and the next to leading muon. The efficiency is also influenced by the slepton mass and the difference between slepton and neutralino masses. To compensate these effects, the final cut applied on the leading muon  $p_T$  has been made dependent of  $M_{\tilde{\mu}} - M_{\tilde{\chi}_0^1}$  as stated in section II B.

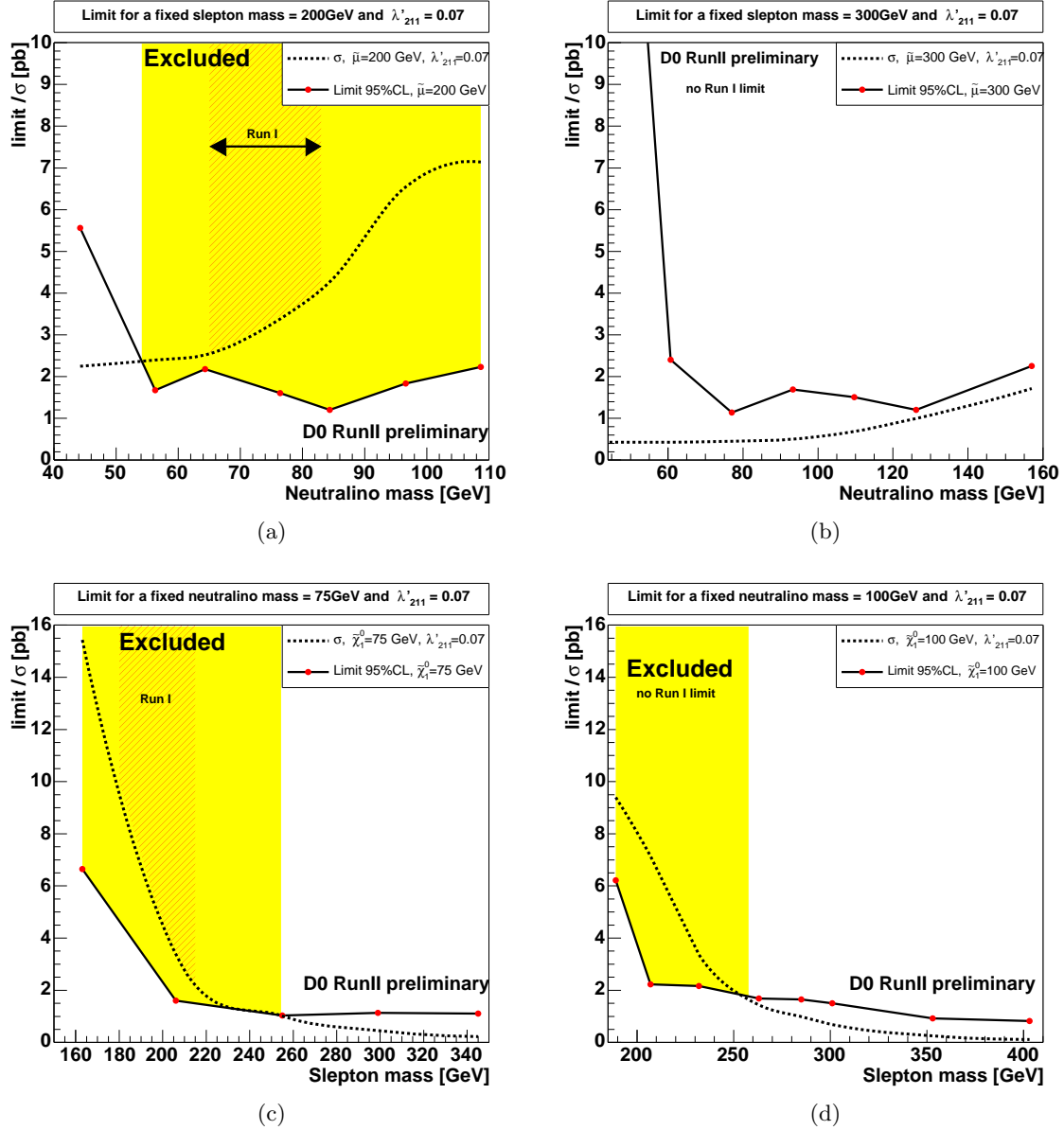


FIG. 3: Cross section and 95% CL limits for fixed slepton masses 200 GeV (a) and 300 GeV (b) and for fixed neutralino masses 75 GeV (c) and 100 GeV (d). The solid yellow area can be excluded for the specified masses and a coupling of  $\lambda'_{211} = 0.07$ . The red hatched area is excluded by the  $D\bar{O}$  Run I analysis [1].

## B. Limits

In the absence of an excess in the data, we set cross section limits on the resonant production of smuons as a function of  $M_{\tilde{\mu}}$  and  $M_{\tilde{\chi}_0^1}$  for the chosen set of parameters  $A_0 = 0$ ,  $\tan(\beta) = 2$  and  $\text{sgn}(\mu) = -1$ . To that end, 95% confidence limits are calculated [10] with the acceptances from each of the simulated signal points.

In Fig. 3 (a) - (b) we show the calculated limit as a function of  $M_{\tilde{\chi}_0^1}$  for two different values of  $M_{\tilde{\mu}}$  and in Fig. 3 (c) - (d) as a function of  $M_{\tilde{\mu}}$  for two different values of  $M_{\tilde{\chi}_0^1}$ . The solid yellow area can be excluded for the specified masses and a coupling of  $\lambda'_{211} = 0.07$ . This area would grow with a larger coupling  $\lambda'_{211}$ . The red hatched area is excluded by the  $D\bar{O}$  Run I analysis [1].

The neutralino production cross section (dashed line), shown in Fig. 3 (a) - (b), is rising until the neutralino mass reaches approximately half of the slepton mass, in this case  $M_{\tilde{\mu}} = 200$  GeV. The reason for this behaviour is the growing branching ratio  $\Gamma(\tilde{\mu} \rightarrow \tilde{\chi}_1^0 + \mu)$ . The ratio grows, since the decay of  $\tilde{\mu}$  into a chargino  $\tilde{\chi}^\pm$  or a neutralino

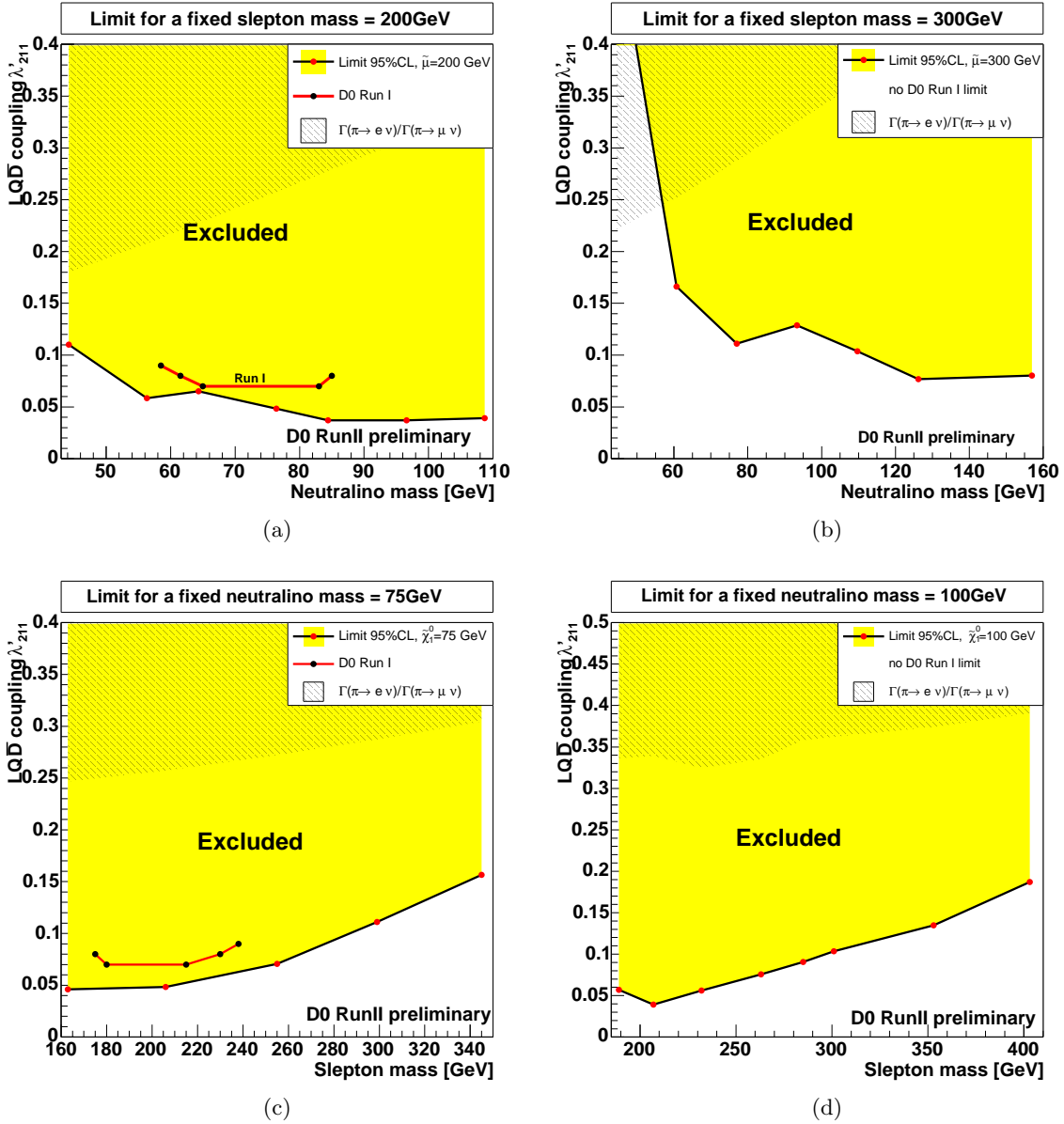


FIG. 4: 95% CL limits on the  $LQ\bar{D}$  coupling  $\lambda'_{211}$  for fixed slepton masses 200 GeV (a) and 300 GeV (b) and for fixed neutralino masses 75 GeV (c) and 100 GeV (d). The solid yellow area can be excluded for the specified masses. The red graph is the limit set by the  $D\bar{O}$  Run I analysis [1] for  $\lambda'_{211} = 0.07, 0.08$  and  $0.09$ . The left hatched limit is obtained from the lepton universality in the pion decays [4].

$\tilde{\chi}_{2,3,4}^0$  becomes more and more kinematical unlikely as these masses are about twice the mass of the 1<sup>st</sup> generation neutralino  $M_{\tilde{\chi}^\pm} = M_{\tilde{\chi}_2^0} \approx 2 \cdot M_{\tilde{\chi}_1^0}$ .

In Fig. 4 we show the exclusion limits on the  $LQ\bar{D}$  coupling  $\lambda'_{211}$  as a function of  $M_{\tilde{\chi}_1^0}$  (a) - (b) and  $M_{\tilde{\mu}}$  (c) - (d). The  $D\bar{O}$  Run I limit (red line) is plotted for  $\lambda'_{211} = 0.07, 0.08$  and  $0.09$ . The limit obtained from lepton universality in pion decays [4] is plotted left hatched.

## VI. CONCLUSION

We have searched for R-parity violating production and decay of charged sleptons in final states with two jets and at least two muons. Using 153.8/pb of integrated luminosity, agreement between the data and the Standard Model

Point	$m_0$ [GeV]	$m_{1/2}$ [GeV]	$M_{\tilde{\mu}}$ [GeV]	$M_{\tilde{\chi}_0^1}$ [GeV]	$\sigma \times \text{BR}$ [pb]	Data	Standard Model	Signal	Limit [pb]
1	190	100	205	44.2	2.2	0.0	$0.6 \pm 0.2^{+0.3}_{-0.1}$	$1.2 \pm 0.3^{+0.3}_{-0.5}$	5.6
2	180	130	204	56.3	2.4	0.0	$0.8 \pm 0.3^{+0.3}_{-0.2}$	$4.1 \pm 0.6^{+1.6}_{-0.5}$	1.7
3	160	180	206	76.4	3.4	0.0	$1.6 \pm 0.4^{+0.7}_{-0.2}$	$6.0 \pm 0.7^{+1.7}_{-1.7}$	1.6
4	130	230	208	96.6	6.5	0.0	$1.6 \pm 0.4^{+0.1}_{-0.2}$	$10.1 \pm 1.5^{+1.7}_{-1.2}$	1.8
5	100	260	207	108.7	7.1	0.0	$1.4 \pm 0.3^{+0.4}_{-0.1}$	$9.1 \pm 1.5^{+0.5}_{-1.8}$	2.2
6	280	140	298	60.7	0.4	0.0	$0.1 \pm 0.0^{+0.0}_{-0.0}$	$0.5 \pm 0.1^{+0.1}_{-0.1}$	2.4
7	270	180	299	77.0	0.5	0.0	$0.1 \pm 0.1^{+0.1}_{-0.1}$	$1.1 \pm 0.2^{+0.2}_{-0.3}$	1.1
8	240	260	301	109.7	0.7	2.0	$0.2 \pm 0.1^{+0.3}_{-0.1}$	$2.6 \pm 0.3^{+0.2}_{-0.4}$	1.5
9	161	375	304	157.0	1.7	1.0	$0.5 \pm 0.2^{+0.0}_{-0.0}$	$7.2 \pm 1.3^{+0.6}_{-1.2}$	2.3
10	220	180	255	76.7	1.0	0.0	$1.0 \pm 0.3^{+0.3}_{-0.1}$	$2.8 \pm 0.3^{+0.2}_{-0.6}$	1.0
11	320	180	345	77.2	0.2	0.0	$0.1 \pm 0.0^{+0.0}_{-0.0}$	$0.6 \pm 0.1^{+0.0}_{-0.1}$	1.1
12	48	261	189	108.9	9.4	1.0	$1.1 \pm 0.3^{+0.2}_{-0.1}$	$19.2 \pm 4.3^{+2.8}_{-4.7}$	6.2
13	305	255	353	108.0	0.2	0.0	$0.1 \pm 0.0^{+0.0}_{-0.1}$	$1.9 \pm 0.2^{+0.1}_{-0.4}$	0.9
14	200	243	263	102.4	1.4	2.0	$1.1 \pm 0.3^{+0.2}_{-0.2}$	$4.4 \pm 0.5^{+0.4}_{-1.1}$	1.7
15	362	254	403	107.9	0.1	0.0	$0.0 \pm 0.0^{+0.0}_{-0.1}$	$1.0 \pm 0.1^{+0.0}_{-0.1}$	0.8

TABLE IV: For each mSUGRA parameter set, the signal cross section, the observed number of events in the data, the expected number of events from Standard Model processes, the expected number of signal events, and the 95% confidence limit for the cross section. For all points the mSUGRA parameters  $A_0 = 0$ ,  $\tan(\beta) = 2$  and  $\text{sgn}(\mu) = -1$  are fixed.

expectation is observed, and limits as a function of  $m_{\tilde{\chi}_1^0}$  and  $m_{\tilde{\mu}}$  have been set.

### Acknowledgments

We thank the staffs at Fermilab and collaborating institutions, and acknowledge support from the Department of Energy and National Science Foundation (USA), Commissariat à l’Energie Atomique and CNRS/Institut National de Physique Nucléaire et de Physique des Particules (France), Ministry of Education and Science, Agency for Atomic Energy and RF President Grants Program (Russia), CAPES, CNPq, FAPERJ, FAPESP and FUNDUNESP (Brazil), Departments of Atomic Energy and Science and Technology (India), Colciencias (Colombia), CONACyT (Mexico), KRF (Korea), CONICET and UBACyT (Argentina), The Foundation for Fundamental Research on Matter (The Netherlands), PPARC (United Kingdom), Ministry of Education (Czech Republic), Natural Sciences and Engineering Research Council and WestGrid Project (Canada), BMBF (Germany), A.P. Sloan Foundation, Civilian Research and Development Foundation, Research Corporation, Texas Advanced Research Program, and the Alexander von Humboldt Foundation.

- 
- [1] DØ Collaboration, V. Abazov *et al.* Phys. Rev. Lett. **89**, 261801 (2002)
  - [2] S. Dimopoulos and L.J. Hall, Phys. Lett. **B 207**, 210 (1988), H. Dreiner and G. G. Ross, Nucl. Phys. **B 365**, 597 (1991)
  - [3] H. Dreiner, published in *Perspectives on Supersymmetry*, ed. by G.L. Kane, World Scientific (1998), hep-ph/9707435
  - [4] B. C. Allanach, A. Dedes, H. K. Dreiner, hep-ph/9906209 (2004);  
F. Ledroit, G. Sajot, GDR-S-008 (ISN, Grenoble, 1998);  
V. Barger, G.F. Giudice, T. Han, Phys. Rev. D **40**, 2987 (1989)
  - [5] F. Déliot, G. Moreau, C. Royon, Eur.Phys.J. **C19**, 155 (2001)
  - [6] F. Déliot, G. Moreau, C. Royon, E. Perez and M. Chemtob, Phys. Lett. **B475**, 184 (2000), H. Dreiner, P. Richardson and M. H. Seymour, hep-ph/0007228
  - [7] T. Sjöstrand *et al.*, Comp. Phys. Comm. **135** 238 (2001); T. Sjöstrand *et al.*, hep-ph/0108264
  - [8] R. Hamberg, W.L. van Neerven and T. Matsuura, Nucl. Phys. **B359**, 343 (1991)
  - [9] N. Ghobbane, S. Katsanevas, P. Morawitz, E. Perez, SUSYGEN 3, hep-ph/9909499
  - [10] T. Hebbeker, *Calculating Upper Limits with Poisson Statistics*, L3 note 2633,  
<http://www.physik.rwth-aachen.de/~hebbeker/l3note-2633.ps> (2001)